The Journal of Neuroscience, July 1990, 10(7): 2373–2384

The Process of Reinnervation in the Dentate Gyrus of Adult Rats: Time Course of Increases in mRNA for Glial Fibrillary Acidic Protein

Oswald Steward, Enrique R. Torre, Linda L. Phillips,[a] and Patricia A. Trimmer

Departments of Neuroscience and Neurological Surgery, University of Virginia Health Sciences Center, Charlottesville, Virginia 22908

The present study evaluates the time course of increased expression of the mRNA for glial fibrillary acidic protein (GFAP) within the dentate gyrus and hippocampus after unilateral lesions of the entorhinal cortex. Levels of GFAP mRNA were evaluated by dot blot hybridization of mRNA isolated from the hippocampus and quantitative *in situ* hybridization. For dot blot hybridization, RNA was isolated from pooled hippocampi obtained from animals killed at 12 hr, 1, 2, 4, 6, 8, 10, 14, and 30 d postlesion. A separate set of animals killed at 2, 4, 6, 8, 10, 12, 14, and 32 d were prepared for *in situ* hybridization. The dot blot analyses of mRNA isolated from the hippocampus revealed that on the side ipsilateral to the lesion, the levels of GFAP mRNA increased rapidly, reaching a peak at 2 d postlesion. The increases were not evident by 12 hr postlesion, but by 24 hr, levels of GFAP mRNA were 5-fold higher than control, and by 48 hr, the levels were over 6-fold higher than control. The levels of GFAP mRNA decreased after 2 d postlesion. At 4 and 6 d postlesion the levels were about 2-fold higher than control. At later postlesion intervals, mRNA levels were comparable to the control. At 2 d postlesion, the levels of GFAP mRNA were also increased about 2-fold over control levels on the contralateral side. After 2 d, the levels of GFAP mRNA on the contralateral side were comparable to the control. *In situ* hybridization revealed a complex pattern of changes in the levels of GFAP. At 2 d postlesion, the levels of GFAP mRNA increased dramatically throughout the hippocampus bilaterally. The increases were most pronounced in the denervated portions of the neuropil; however, the levels of GFAP mRNA were also substantially elevated in laminae that do not receive direct projections from the entorhinal cortex. GFAP mRNA levels were also increased in other areas that receive projections from the entorhinal cortex, including the septum, lateral-dorsal thalamus, and entorhinal cortex contralateral to the lesion. In addition, GFAP mRNA levels were increased in regions bordering the ventricles throughout the brain, and over the surface of the tectum. After 2 d postlesion, the increases in the levels of GFAP mRNA were for the most part restricted to areas containing terminal degeneration. The generalized increases throughout the hippocampus were no longer apparent. Areas bordering the ventricles continued to exhibit higher labeling than in control animals, but this effect was not as prominent as at 2 d postlesion. The persistent increases in GFAP mRNA within the denervated laminae presumably reflect some of the cellular events involved in reactive gliosis in areas containing degeneration debris. The rapid transient increases in GFAP mRNA in nondenervated areas must occur in response to some other signal. Increases in periventricular zones and over the surface of the tectum may reflect the action of some diffusable factor, whereas increases within the hippocampus may reflect a change in expression due to changes in physiological activity.

One of the best-characterized examples of synaptic reorganization after injury to the CNS is that which occurs in the dentate gyrus following damage to the projections from the entorhinal cortex. Following destruction of normal inputs, several surviving afferent systems participate in the reinnervation of the dentate granule cells (for a review, see Cotman and Nadler, 1978). Because this process has been so well characterized in terms of the cellular participants, it can potentially serve as a useful system in which to define the cellular and molecular events associated with the lesion-induced growth process (Steward, 1986).

One clue about the molecular events associated with the lesion-induced growth has come from studies of protein synthesis within the denervated dentate gyrus. Using autoradiographic methods, we have detected increases in protein synthesis within the denervated neuropil of the dentate gyrus during the period of synapse replacement (Fass and Steward, 1983; Phillips et al., 1987). The increases in incorporation were first apparent at about 4 d postlesion and reached a peak at 6–8 d. Because of the close temporal relationship between the increases in protein synthesis and the early phases of the reinnervation process, we proposed that the increases in the synthesis of some protein(s) within the dendritic laminae may play an important role in the reinnervation process. For this reason, we have been interested in defining the protein species that are synthesized within the denervated neuropil.

One line of circumstantial evidence suggests that the increased incorporation within the denervated neuropil may reflect protein synthesis within dendrites. This hypothesis is based on the

Received Nov. 27, 1989; revised March 5, 1990; accepted March 12, 1990.

Thanks to Leanna Whitmore and Roshna Wunderlich for their excellent technical help, to N. Cowan for the gift of the cDNA clone for GFAP, to D. Chikaraishi for recloning the cDNA clone into a riboprobe vector, to Ted Mifflin and the staff of the Molecular Probe Laboratory of the University of Virginia for producing the labeled cRNA probes used in this study, and to Peter Meeberg and Aryeh Routtenberg for their help in developing the techniques for *in situ* hybridization. Supported by NIH Grant NS12333 to O.S. Tissue culture studies and probe preparation was supported in part by NIH Grant NS20255 to P.A.T.

Correspondence should be addressed to Dr. Oswald Steward, Department of Neuroscience, Box 230, University of Virginia Health Sciences Center, Charlottesville, VA 22908.

[a] Present address: Department of Neurosurgery, Medical College of Virginia, Richmond, VA 23298.

fact that the increases in protein synthesis occur concurrently with increases in polyribosomes beneath spine synapses (Steward, 1983). However, it is also possible that some or all of the increased incorporation reflects an increased synthesis of protein by reactive astrocytes. It is well known that astrocytes within the denervated neuropil undergo a substantial hypertrophy following entorhinal cortical lesions (Rose et al., 1976; Gage et al., 1988). This glial response is thought to play an important role in the reinnervation process. Astrocytes are almost certainly responsible for clearing degenerating synaptic terminals from the postsynaptic neuron (Matthews et al., 1976). They may also contribute to neuronal growth directly by producing growth factors (Nieto-Sampedro et al., 1982, 1983; Needels et al., 1986). For these reasons, it is of considerable interest to directly evaluate the molecular events within reactive astrocytes during the period of lesion-induced synapse turnover.

If the increases in protein synthesis within the denervated neuropil reflect synthesis by reactive astrocytes, then one would expect increases in the synthesis of glial proteins during the period of increased incorporation. Thus, the present study evaluates the time course of increases in the mRNA for glial fibrillary acidic protein (GFAP), a protein that is unique to astrocytes and up-regulated in reactive astrocytes (Tetzlaff et al., 1988). Levels of GFAP mRNA are evaluated within the denervated dentate gyrus using dot blot and quantitative *in situ* hybridization techniques. Our results reveal dramatic increases in GFAP mRNA within the denervated dentate gyrus and in other regions that would be denervated following damage to the entorhinal cortex. However, the increases in GFAP mRNA occurred with a different time course than the increases in protein synthesis in the denervated neuropil. Our results also reveal that there are increases in GFAP mRNA in nondenervated zones in the hippocampus and in other brain regions, including the surface of the tectum and periventricular areas throughout the brain. These results define the time course of changes in astrocyte gene expression following injury and the relationship between glial reactivity and reactive synaptogenesis. In addition, the present results provide clues about the signals that regulate GFAP expression.

Materials and Methods

A total of 43 adult male Sprague-Dawley rats (300–350 gm) received unilateral lesions of the entorhinal cortex using a procedure that has been described previously (Loesche and Steward, 1977). Two separate dot blot analyses were carried out. In the first, RNA was isolated from animals killed at 2, 4, 6, 8, 10, 14, and 30 d postlesion (2 animals at each time point). Two control animals were also prepared. Because we found that peak levels of GFAP mRNA were observed at 2 d postlesion, a second analysis was carried out to define the onset of the response. For this purpose, RNA was isolated from control animals and from animals killed at 12, 24, and 48 hr postlesion (3 animals per time point). Animals were killed for *in situ* hybridization at 2, 4, 6, 8, 10, 12, 14, and 32 d postlesion (2 animals at each time point). Two control animals were also prepared.

Probe preparation. The probes used in this study were derived from a cDNA for mouse GFAP that has been characterized previously (Lewis et al., 1984). The original cDNA clone was 2.5 kilobases (kb) in length, which specified over 97% of the GFAP amino acid sequence, and also included a 1.4 kb long portion of the 3′ untranslated region. This original 2.5 kb cDNA was cut using the restriction enzyme Hind III, to obtain a 1.26 kb fragment from the 5′ (coding) portion of the original cDNA clone. This 1.26 kb fragment was recloned into the Hind III site of a Bluescript m13-vector by D. Chikaraishi (Tufts University). Samples of the Bluescript plasmid with the GFAP insert were provided to us as a gift.

Large-scale preparation of the plasmids with the GFAP insert was carried out by the Molecular Probe Laboratory of the University of Virginia. Circular plasmids were isolated using standard procedures and linearized with the restriction enzyme PVU II. Because there is a PVU II site within the GFAP cDNA, the restriction enzyme splits the GFAP cDNA into 2 fragments. This allowed the production of an antisense probe of about 1000 bases in length and a sense probe of about 250 bases in length. ^{35}S-labeled sense and antisense probes were produced from this vector as described in Maniatis et al. (1983). T3 promoter was used to produce antisense probes, and T7 was used to produce sense probes. The specific activity of the antisense probes ranged from 3.1×10^8 to 5.6×10^8 cpm/μg of RNA (average = 4.3×10^8). Because the sense probe was much shorter than the antisense, we also used a sense cRNA produced from a cDNA for protein F1 as a control; this cRNA was about 740 bases in length. The use of antisense and sense cRNAs produced from the F1 clone has been described previously (Rosenthal et al., 1987).

mRNA isolation. To characterize the specificity of the cRNA probes, RNA was isolated from whole hippocampi by guanidinium isothiocyanate extraction followed by CsCl gradient centrifugation (Chirgwin et al., 1979; Ausubel et al., 1987). Five micrograms of total cellular RNA was separated electrophoretically on denaturing 1.4% agarose-glyoxal gels. The gels were equilibrated for 30 min in 0.5× SSC, and the RNA was transferred to a nylon (Nytran) membrane (Wahl et al., 1981; Maniatis et al., 1983). The membranes were hybridized at 65°C for 24 hr with approximately 2.5 ng/ml of the ^{35}S-labeled probes (1×10^6 cpm/ml). The hybridization buffer was 50% formamide, 5× SSPE, 5× Denhardts solution, 1% SDS, 100 μg/ml of tRNA, and 100 μg/ml of polyA. The blot was washed 3× (15 min each) in 1× SSPE/1% SDS at 65°C, treated with RNAse (10 μg/ml in 5× SSC) for 1 hr at 40°C, washed for 1 hr at 60°C in 0.1× SSPE with 1% SDS, and dried. The membrane was then exposed to Kodak X-Omat AR film at −70°C for 72 hr (Maniatis et al., 1983).

Dot blot analyses. To obtain RNA for the dot blot analyses, animals were deeply anesthetized with sodium pentobarbital and decapitated, and the hippocampi were rapidly removed. Total cellular RNA was isolated from hippocampi ipsilateral and contralateral to the lesion as described above. The hippocampi from the 2–3 animals at each time point were pooled in order to obtain sufficient material for RNA isolation. The total cellular RNA was dissolved in 10× SSC, 7.5% formaldehyde (pH 7.4), and incubated at 65°C for 10 min. Ribosomal RNA was isolated by oligo-DT column chromatography from a separate sample of total RNA obtained from whole rat forebrains. Ribosomal RNA was defined as the fraction that does not bind to the oligo-DT column.

Samples of RNA were applied to a Biorad manifold and filtered through a Nytran membrane. The membrane was washed in 10× SSC and dried, and the RNA was fixed to the membrane by cross-linking with ultraviolet light (Wahl et al., 1981). Hybridization was carried out as described above. The membranes were then treated with RNAse (10 μg/ml in 5× SSC) and washed in a "high stringency" buffer. For the first experiment, the membranes were treated with RNAse for 1 hr at 40°C. For the second experiment, the RNAse treatment was for 30 min at 35°C. The latter treatment protocol resulted in higher specific labeling without an increase in background. The membranes were then dried and exposed to Kodak X-Omat film. The total amount of radioactivity in each spot was evaluated by scintillation counting.

To evaluate the linearity of probe binding with increasing concentrations of RNA, samples of RNA from control animals were spotted at concentrations of 1, 2, 4, and 8 μg per spot. Near-asymptotic binding was obtained using using 4 μg samples (see Fig. 1). Thus, for subsequent dot blot analyses, triplicate samples containing 4 μg of RNA were spotted. As a control for nonspecific binding, we evaluated the extent of hybridization to sections of the nylon membrane with no added RNA (blank) and the extent of hybridization to ribosomal RNA. There was little binding of the probe to the blank, and the levels of hybridization to ribosomal RNA were only slightly higher than the blank (see Fig. 2).

In situ *hybridization.* Animals to be prepared for *in situ* hybridization were perfused with 4% paraformaldehyde in 0.1 M phosphate buffer while deeply anesthetized with sodium pentobarbital. The brains were removed and immersed in 15% sucrose in 4% paraformaldehyde/phosphate buffer for 1–4 hr. The brains were mounted on the chuck of a cryostat and frozen by immersion in methyl butane chilled with liquid nitrogen. The brains were sectioned at 20 μm in the horizontal plane using a cryostat, and the sections were thaw-mounted onto polylysine-coated microscope slides. A total of 150–200 sections were collected throughout the dorsoventral extent of the hippocampus for each animal.

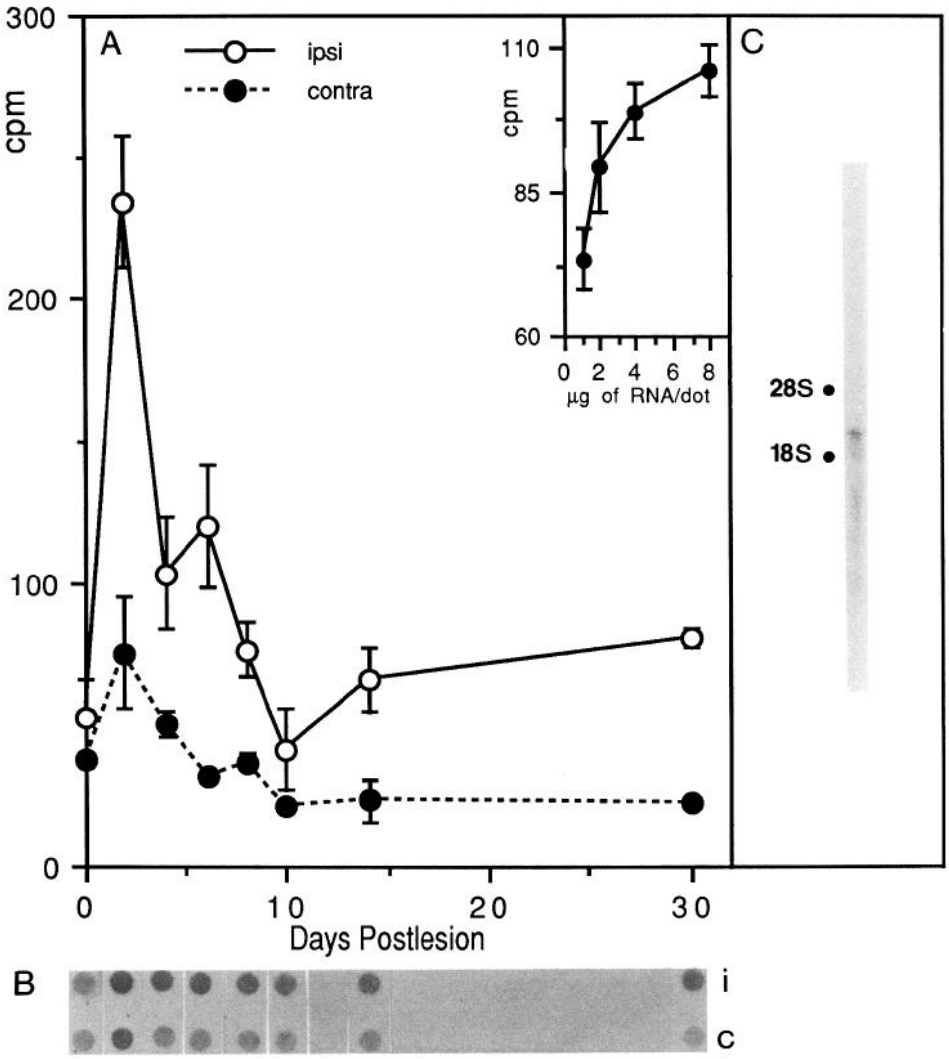

Figure 1. Time course of increases in GFAP mRNA in the denervated dentate gyrus as measured by dot blot hybridization. *A,* RNA was obtained from pooled hippocampi from 2 animals per time point (ipsilateral and contralateral to an entorhinal cortical lesion). Triplicate samples containing 4 µg of RNA were spotted onto nylon membranes, and the membranes were hybridized with ^{35}S-labeled probes for GFAP mRNA. The *graph* illustrates the mean cpm/dot (±SD) from the hippocampus ipsi- and contralateral to the lesion at 2, 4, 6, 8, 10, 14, and 30 d postlesion. The *inset* illustrates that the extent of hybridization to RNA from control animals increases as a function of the amount of RNA that is spotted. Each value represents the mean and range of values from 2 separate mRNA preparations from the control animals. The increase in labeling is nonlinear after the amount of RNA per spot exceeds 4 µg. For this reason, the 4 µg concentration was used for all quantitative assessments. *B,* The lower portion of the figure illustrates a film autoradiograph of the dot blots of RNA from ipsilateral and contralateral sides. *C,* mRNA from whole brain was separated on an agarose gel and transferred to nylon membranes. The membranes were hybridized with the ^{35}S-labeled probes for GFAP mRNA, and the northern blots were exposed to X-ray film. The *fluorograph* illustrates that the probes hybridize to a single band on the RNA gels. There is no detectable binding to ^{18}S or ^{28}S RNA.

The slides were then divided into sets composed of 1 slide out of each 15 (a 1-in-15 series) from the total collected from each case. The slides were stored frozen at −80°C prior to use.

In situ hybridization was carried out using the procedure described in Rosenthal et al. (1987). The slides were allowed to warm to room temperature and were then postfixed for 10 min in 4% paraformaldehyde in phosphate buffer. The slides were pretreated with proteinase K (1 µg/ml in RNAse buffer) for 10–30 min, washed in 0.5× SSC, dried carefully with a Kimwipe, and placed flat on 3-mm-thick glass bars in a 150 mm Petri dish kept humid with a formamide-containing buffer. The sections were covered with 100 µl of hybridization buffer (without the probe) and incubated for 1–3 hr at 42°C. A 20 µl aliquot of hybridization buffer containing 1–2 µl of probe (about 3 × 10^5 cpm) and 2 µg of tRNA was added to the hybridization buffer after heat treatment for 3 min at 95°C. A 22 × 22 mm coverslip was then placed over the hybridization mix. Hybridization was carried out overnight (18–24 hr) at 55°C.

The following day, the coverslips were removed, and the slides were washed in 2× SSC containing 10 mM beta mercaptoethanol (BME) and 1 mM EDTA. The slides were then incubated for 30 min at room temperature in a solution with 500 mM NaCl, 10 mM Tris pH 8.0, and 2 µg/ml RNAse. The slides were washed for 2 hr at 55°C in a "stringency" buffer containing 0.1× SSC, 10 mM BME, and 1 mM EDTA. Finally, the sections were dehydrated in graded ethanols in 0.3 M ammonium acetate, and dried. For autoradiography, slides were dipped in Kodak NTB2 emulsion diluted 1:1 with water. The autoradiographs were exposed for 2 weeks, developed in Kodak D19, and stained with Cresyl violet.

Mixed cultures of neurons and glia derived from the dentate gyrus were also prepared for *in situ* hybridization in order to evaluate the specificity of labeling for astrocytes. Dentate gyri were dissected from 6-d-old rat pups and enzymatically dissociated using trypsin. The dissociated cells were plated on polylysine-coated coverslips and maintained in a high-potassium medium (Burry, 1983). The neurons that survive in such cultures are presumably primarily granule neurons. Cells that had been maintained in culture for 7–14 d were fixed with 4% paraformaldehyde in phosphate buffer and stored in 70% alcohol at 4°C prior to use. Prior to hybridization, coverslips were incubated in 0.1 M phosphate buffered saline with 5 mM $MgCl_2$ for 10 min, washed in 0.2 M Tris (pH 7.4) with 0.1 M glycine, and then incubated in 2× SSC/50% formamide (Lawrence and Singer, 1986). Essentially the same protocol was used for the *in situ* hybridization, making only the modifications necessary to handle material affixed to coverslips instead of slides.

After hybridization, the coverslips were immunostained for beta-tubulin and GFAP using fluorescent secondary antibodies in order to visualize neurons and glia (P. A. Trimmer and O. Steward, unpublished observations). The antibody to beta-tubulin has been described previously (Caceres et al., 1983). The antibody to GFAP was obtained from Accurate Chemical and Scientific Corporation. Following overnight incubation in the primary antibodies (1:200 dilution), the cells were washed with PBS, and incubated for 30 min in fluorescein isothiocyanate (FITC)

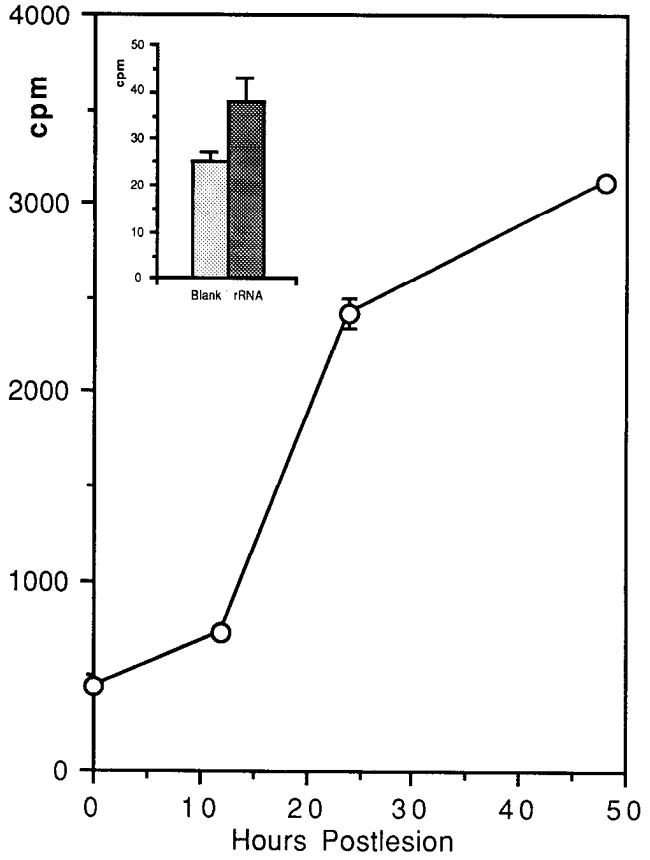

Figure 2. Induction of GFAP mRNA occurs within 24 hr postlesion. To determine the onset of the increases in GFAP mRNA, levels of GFAP mRNA were evaluated in animals killed at 12, 24, and 48 hr postlesion (3 animals per time point). Quadruplicate samples of 4 μg of RNA were spotted onto nylon membranes and hybridized with ^{35}S-labeled GFAP probe. The *graph* illustrates the mean cpm/spot (±SD). The *inset* illustrates the extent of probe binding to the nylon membrane without added RNA (*blank*), and to spots containing approximately 4 μg of ribosomal RNA (RNA that does not bind to an oligo-DT column). The overall level of labeling is higher in this dot blot than in Figure 1 because the posthybridization RNAse treatment was shorter (30 min at 35°C vs. 1 hr at 40°C for the blot in Fig. 1).

or rhodamine-conjugated secondary antibodies (1:100 dilution). The cells were then air-dried and prepared for autoradiography as described above.

Results

Specificity of the ^{35}S riboprobes was evaluated by Northern blot analysis using mRNA obtained from whole forebrain. As illustrated in Figure 1, the riboprobes recognized a single band on the gels at an apparent molecular weight of around 2.6 kb. There was no evidence of binding to either ^{18}S or ^{28}S RNA. This is consistent with previous studies using probes prepared from this vector (Lewis et al., 1984).

Dot blot analyses of GFAP mRNA levels after lesions of the entorhinal cortex

Quantification of GFAP mRNA levels in whole hippocampus by dot blot hybridization revealed that there were substantial increases in the levels of GFAP mRNA in the hippocampus after lesions of the entorhinal cortex (Fig. 1). Ipsilateral to the lesion, the increases were most pronounced at 2 d postlesion, when GFAP mRNA levels were about 5–6-fold higher than in unoperated controls. At 4 and 6 d postlesion, GFAP mRNA levels were about 2-fold higher than control. Thereafter, the levels of GFAP mRNA decreased toward control levels. In the hippocampus contralateral to the lesion, there were also increases in GFAP mRNA at 2 d postlesion; however, the extent of the increase was much less than on the ipsilateral side. The levels of GFAP mRNA on the contralateral side returned to near control levels by 4 d postlesion.

Because GFAP mRNA levels were at their peak at the earliest time point examined in the first experiment, a second analysis was carried out to define the onset of the response. The levels of GFAP mRNA in the hippocampus ipsilateral to the lesion were evaluated by dot blot analysis of RNA isolated from animals killed at 12, 24, and 48 hr postlesion (3 animals per time point). The mRNA from control animals was from the same sample of RNA that was used for Figure 1. As illustrated in Figure 2, GFAP mRNA levels increased almost 2-fold by 12 hr postlesion, and by 24 hr GFA mRNA levels had increased about 5-fold. As in the previous experiment, the levels of GFAP mRNA were about 6-fold higher than control by 48 hr. The overall level of labeling in the dot blot analysis illustrated in Figure 2 was considerably higher than in the 1 illustrated in Figure 1 because of the differences in posthybridization RNAse treatment (see Materials and Methods).

Analysis of GFAP mRNA levels by in situ *hybridization*

The pattern of labeling of mixed cultures of neurons and glia and within sections suggested that the probe specifically labeled astrocytes. As illustrated in Figure 3, in mixed cultures of astrocytes and neurons from the dentate gyrus, labeling was restricted to flat cells that have the morphological appearance of astrocytes. Immunostains with a GFAP antibody revealed that most of these flat cells are GFAP positive (data not shown). Only background levels of labeling were observed over the neurons. These results are consistent with previous studies that show selective labeling of astrocytes in culture using cDNA probes derived from this vector (Holmes et al., 1988).

In tissue sections from control animals, the labeling for GFAP mRNA was fairly uniform throughout the brain. Grain density was slightly higher over the glia limitans at the brain surface (Fig. 4). In the hippocampus, labeling was slightly higher over fiber tracts (for example, the alveus) and in stratum lacunosum moleculare of CA1, where the number of glial cells is higher than in other portions of the neuropil. There was no evidence for labeling over neuronal cell body laminae. In neuropil layers, grains appeared to be diffusely distributed. For example, in the molecular layer of the dentate gyrus, grains did not appear to be selectively localized around the nuclei of cells, most of which are presumably glia (Fig. 4*C*). The apparent lack of cellular localization may reflect the low spatial resolution provided by the ^{35}S-labeled probes. However, it is also difficult to determine the distribution of grains over the cytoplasm of individual cells because the cytoplasm was unstained. Nissl staining was restricted to nuclei because of the treatment of the tissue with RNAse.

The analyses of changes in GFAP mRNA after lesions by *in situ* hybridization confirmed the dot blot analyses and revealed some surprising features of the spatial distribution of the increases in message levels. In interpreting the changes in labeling, it is helpful to briefly summarize the pattern of terminal degeneration produced by unilateral entorhinal cortical lesions. The lesions destroyed the entorhinal cortex proper (including the

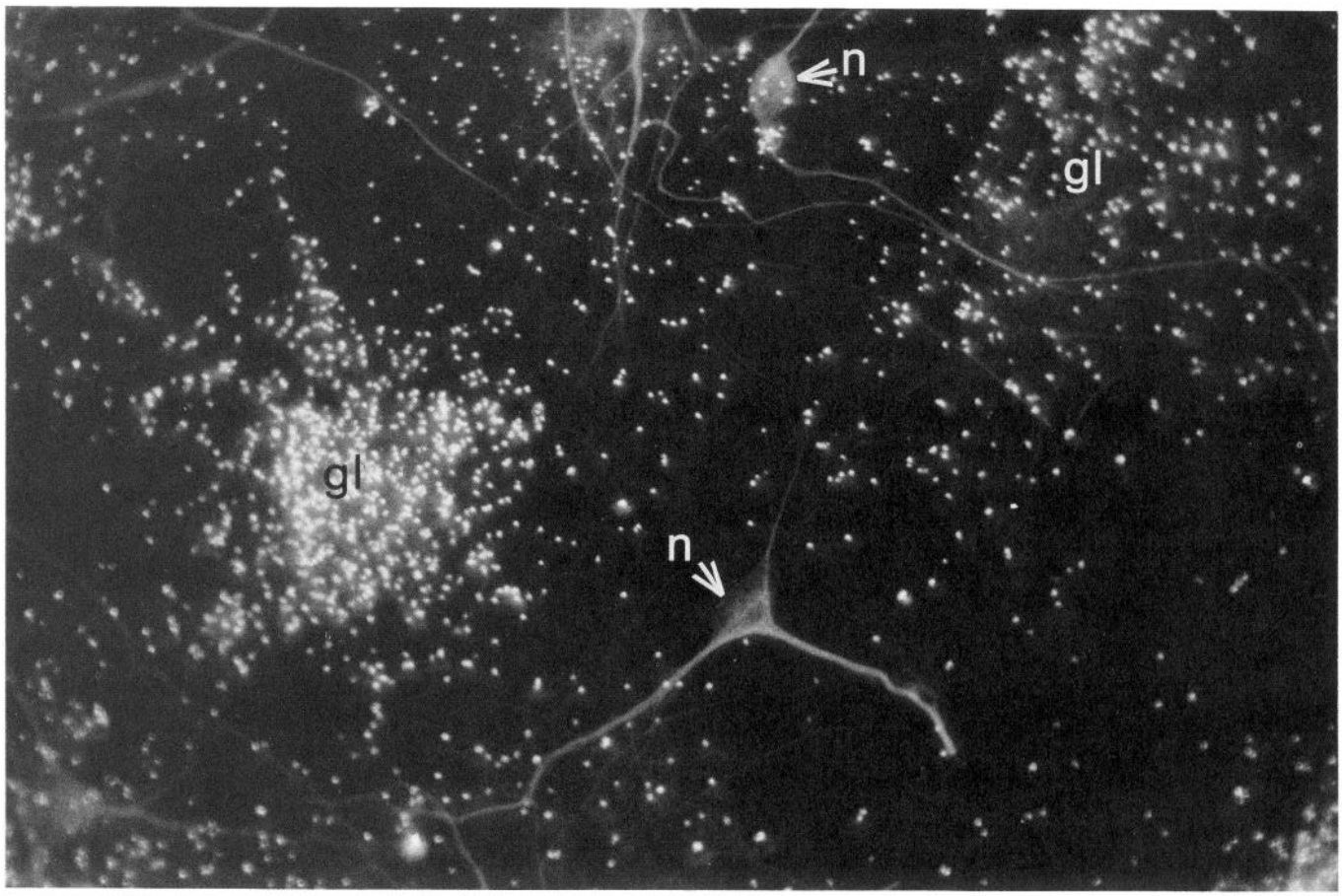

Figure 3. Selective labeling of astrocytes following *in situ* hybridization with ^{35}S-labeled cRNA probes for GFAP. Mixed cultures of neurons and glial cells were prepared from 1–5-d-old rat hippocampi. Most of these neurons are presumably granule cells. The cultures were hybridized with ^{35}S-labeled probes for GFAP mRNA and then immunostained for tubulin as described in Materials and Methods. Double-exposure fluorescence/dark-field photographs reveal neurons (*n*) and flat cells resembling astrocytes (*gl*). In similar cultures, most such flat cells stain positively for GFAP. The presumed neurons were not labeled by the probe for GFAP, while the presumed astrocytes were heavily labeled.

deep laminae) along with the presubiculum, parasubiculum, and sometimes portions of the subiculum. In a few animals, the damage extended into the most posterior and ventral portions of the dentate gyrus. Following such lesions, there is dense degeneration debris in the molecular layer of the ipsilateral dentate gyrus and in the stratum lacunosum moleculare of the hippocampus bilaterally (Steward et al., 1974). Other laminae in the hippocampus are for the most part free of degeneration debris. Terminal degeneration is also present in the lateral dorsal thalamus, the septum, the contralateral entorhinal area, and in areas of the neocortex ipsilateral to the lesion.

As illustrated in Figure 5, there were very dramatic increases in labeling for the GFAP probe at 2 d postlesion. There were substantial increases in grain density in all regions that receive direct projections from the entorhinal cortex, including the hippocampus, lateral dorsal thalamus, septum, and contralateral entorhinal area. Surprisingly, however, there were also increases in labeling in areas that would not contain terminal degeneration after such lesions. For example, there were dramatic increases in labeling throughout the hippocampus, both ipsilateral and contralateral to the lesion. Grain density appeared to be highest in the laminae that receive direct projections from the entorhinal cortex (the molecular layer of the dentate gyrus ipsilateral to the lesion, and stratum lacunosum moleculare of CA1 bilaterally). However, grain density within the denervated zones was only slightly higher than in nondenervated laminae.

There were also increases in grain density over the surface of the tectum, particularly ipsilateral to the lesion and in periventricular zones throughout the brain. For example, Figure 5*C* illustrates the increases in labeling surrounding the third ventricle. Similar increases in labeling were observed in the areas bordering the fourth ventricle (data not shown). Interestingly, the areas at the margin of the lesion cavity did not exhibit high levels of labeling at 2 d postlesion.

At 4 d postlesion and thereafter, the pattern of labeling was quite different. Except for the increases in labeling over periventricular zones (see below), the areas exhibiting high levels of labeling coincided with areas that would be expected to contain degeneration debris after unilateral entorhinal cortex lesions. Thus, the areas at the margin of the lesion cavity exhibited heavy labeling, as did the entire posterior cortex ipsilateral to the lesion.

Within the hippocampus, grain density was highest in the molecular layer of the dentate gyrus ipsilateral to the lesion, and within stratum lacunosum moleculare bilaterally (Fig. 6*A*). Labeling in certain nondenervated portions of the hippocampal neuropil (such as the hilus of the dentate gyrus) was also somewhat higher than control, but this effect was not nearly as dra-

matic as at 2 d postlesion. Grain density was also high in other areas that would contain terminal degeneration, including the lateral dorsal thalamus. This same basic pattern of labeling was evident between 6 and 14 d postlesion. However, the density of labeling within the denervated portion of the neuropil appeared to be higher at 8 d than at 4 and 6 d postlesion (Fig. 6*B*). This impression was confirmed by the quantitative analyses (see below). In addition, the density of labeling at the lesion margin also appeared to increase progressively between 4 and 8 d postlesion, and decrease thereafter. This change in labeling was not evaluated quantitatively. By 32 d postlesion, the levels of labeling over the denervated portions of the neuropil were only slightly higher than elsewhere within the section (data not shown).

Throughout the 4–14-d postlesion period, periventricular areas continued to exhibit increased labeling (see, for example, Fig. 6). The increases were restricted to a thin band of labeling adjacent to the ventricle. Qualitatively, the levels of labeling over periventricular zones did not appear to be as high between 4 and 14 d postlesion as at 2 d.

Quantitative analyses

To quantitatively evaluate the time course of the increases in labeling revealed by *in situ* hybridization, grain counts were performed using a Gould IP8500 image analysis system and software developed by the Biomedical Image Processing Center at the University of Virginia. A minimum of 5 slides were chosen for each postlesion interval (2–3 slides per case), selecting sections without folds or wrinkles, and where background labeling was relatively uniform over the slide. Grain density was evaluated over the molecular layer of the dentate gyrus, over the stratum lacunosum moleculare of CA1, and over the stratum radiatum of CA1, making 4–5 separate measurements per site. Stratum radiatum is not innervated by the entorhinal cortex and thus provides a measure of changes in grain density within nondenervated portions of the hippocampal neuropil. In addition, to provide an internal standard for variability in the extent of hybridization from case to case, grain density was evaluated over deep layers of the cerebral cortex on the side contralateral to the lesion.

The quantitative analyses of autoradiograms confirmed the qualitative impressions and the dot blot analyses and provided additional details. Figure 7*A* illustrates the time course of the changes in grain density within denervated zones (the molecular layer of the dentate gyrus ipsilateral to the lesion and stratum lacunosum moleculare bilaterally), while Figure 7*B* illustrates the time course of changes in grain density in the nondenervated zones (the contralateral dentate gyrus and stratum radiatum). As expected, the increases in labeling within all zones were greatest at 2 d postlesion. Within the denervated zones, the level of labeling decreased after 2 d postlesion, but remained much higher than control throughout the 4–14-day postlesion interval. There appeared to be a secondary peak in labeling between 6 and 8 d. By 32 d, the level of labeling was near control levels. Within the nondenervated zones, the largest increases in labeling were at 2 d. The levels of labeling within nondenervated zones were only slightly higher than control levels between 4 and 14 d postlesion.

There are some technical problems that prevent an accurate assessment of grain density in heavily labeled areas. When grain density is very high, it is difficult to resolve individual silver grains. In addition, increases in the number of small, darkly staining cells within denervated zones (presumably microglia) make it more difficult to carry out accurate counts. For these reasons, the quantitative analyses almost certainly underestimate the actual extent of the increases in grain density.

Discussion

The present results reveal dramatic increases in the levels of GFAP mRNA within both denervated and nondenervated zones in the hippocampus after unilateral entorhinal lesions. Increases in labeling were also observed in other brain regions that receive projections from the entorhinal cortex and in periventricular zones throughout the brain.

Reactive gliosis in response to injury has been well characterized in a number of settings, and one of the hallmarks of the reactive change is an increase in GFAP (Bignami and Dahl, 1976; Nathaniel and Nathaniel, 1981; Tetzlaff et al., 1988). In considering the mechanisms that lead to increased production of GFAP, it is useful to consider the different settings in which glial cells become reactive. One well-characterized response occurs at the site of injury (Amaducci et al., 1981; Mathewson and Berry, 1985; Schiffer et al., 1986). There are also well-characterized examples of increases in GFAP within glial cells at a distance from the site of injury, for example, within degenerating nerves (Vaughn et al., 1970; Cook and Wisniewski, 1973), in areas undergoing retrograde degeneration after axotomy (Graeber and Kreutzberg, 1986; Tetzlaff et al., 1988), or, as in the present study, in areas that would be denervated by the lesion (Rose et al., 1976; Barret et al., 1981; Gage et al., 1988).

→

Figure 4. Pattern of labeling of tissue sections from control animals following *in situ* hybridization with ^{35}S-labeled cRNA probes for GFAP. *A*, A horizontal section midway through the brain. *Sept* = septum; *DG* = dentate gyrus; *H* = hippocampus; *EC* = entorhinal cortex; *Thal* = thalamus; *Cb* = cerebellum; *VIII* = the third ventricle. The scale bar in *A* represents 1 mm in *A*, 300 μm in *B*, and 30 μm in *C*.

Figure 5. Increases in GFAP mRNA following unilateral destruction of the entorhinal cortex (2 d postlesion). *A*, Dark-field photograph of a horizontal section through the dorsal portion of the brain. Note that there is increased labeling in the hippocampus bilaterally, and over the surface of the tectum (*SC* and *IC*). The extent of the lesion is illustrated by the *dotted line* on the left (*ECL*). Necrotic tissue is still present in the lesion site at this time, but there is no labeling with the GFAP probe. *DG* = dentate gyrus; *H* = hippocampus; *SC* = superior colliculus; *IC* = inferior colliculus; *slmi* and *slmc* = the stratum lacunosum moleculare of the hippocampus ipsilateral and contralateral to the lesion. *B*, Pattern of labeling in the ventral septum (*Sept*) from the same case as illustrated in *A*. This photograph is of a relatively deep horizontal section. Note increased grain density in the anterior portion of the septum (*arrow*). *C*, Increased grain density in the periventricular zones of the third ventricle (*VIII*). The scale bar represents 1 mm in *A*, and 300 μm in *B* and *C*.

Figure 6. Increases in GFAP mRNA following unilateral destruction of the entorhinal cortex. *A*, 4 d postlesion; *B*, 8 d postlesion. *Unlabeled arrows* indicate the areas of increased labeling within the dentate gyrus, which correspond to the site of degeneration debris resulting from the lesion. Note also the increased labeling within the area of the lesion and at the lesion margins. *LD* = lateral dorsal thalamus. Other abbreviations are as in previous figures. Scale bar, 1 mm.

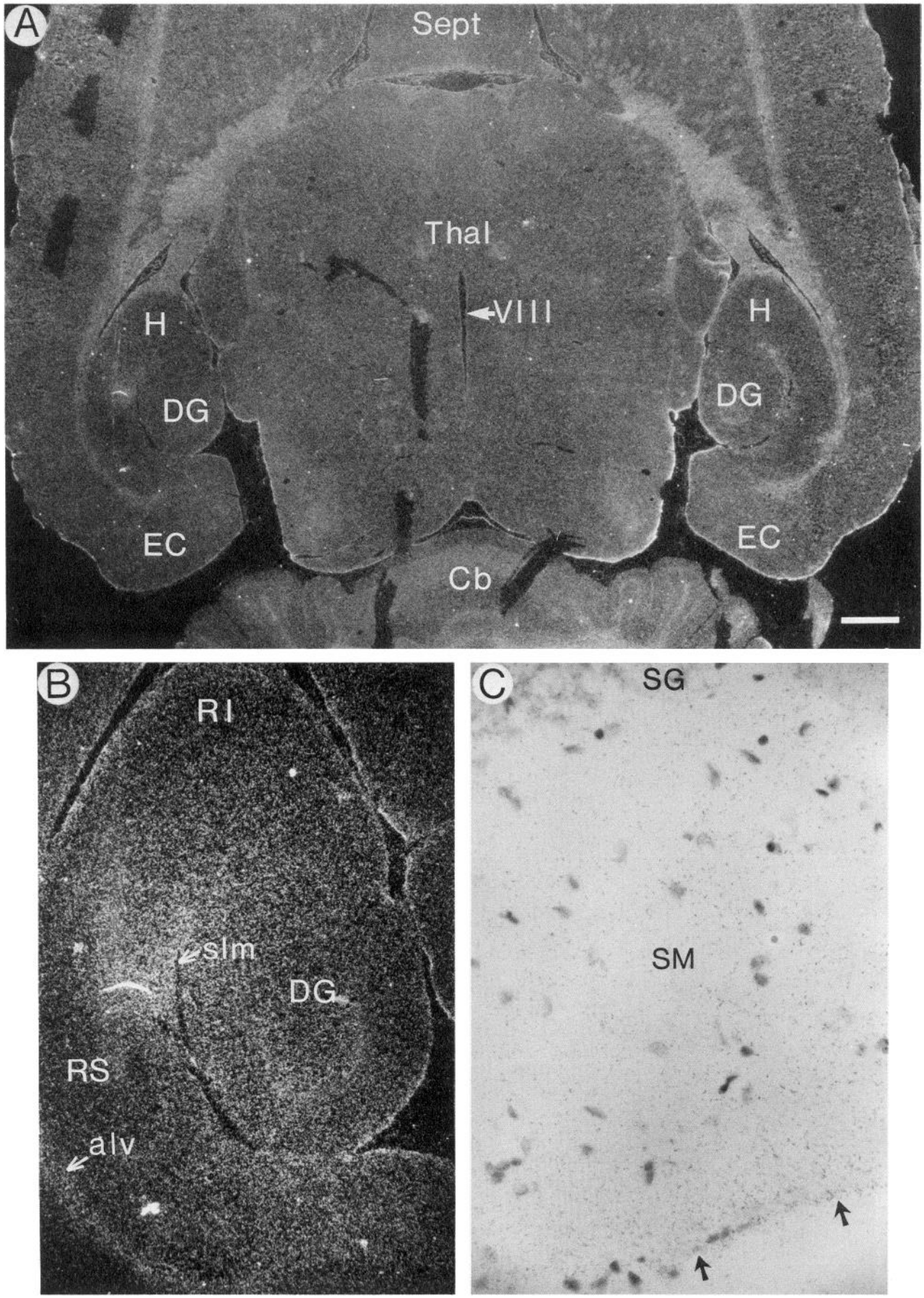
A
Sept
Thal
VIII
H
H
DG
DG
EC
EC
Cb
B
RI
slm
DG
RS
alv
C
SG
SM

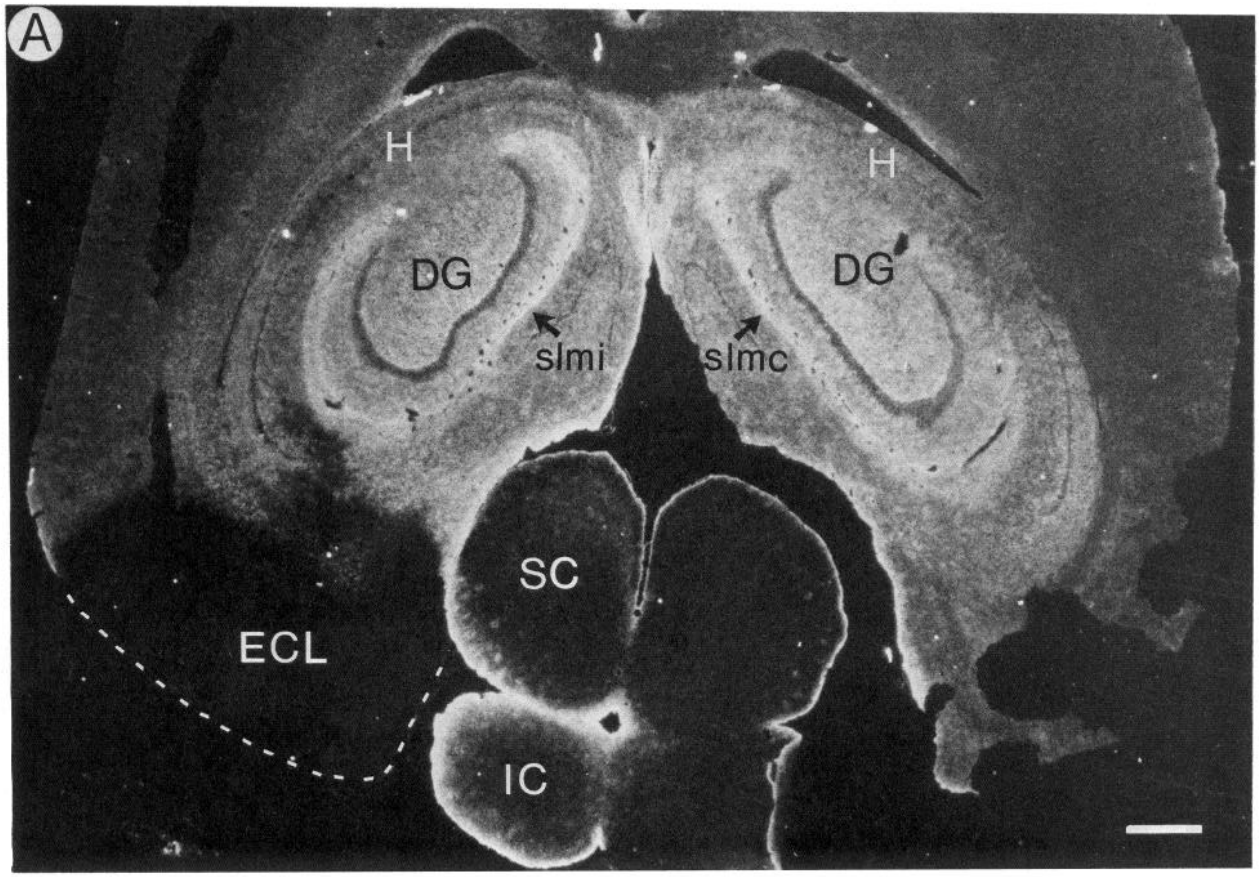
A
H
H
DG
DG
slmi
slmc
SC
ECL
IC

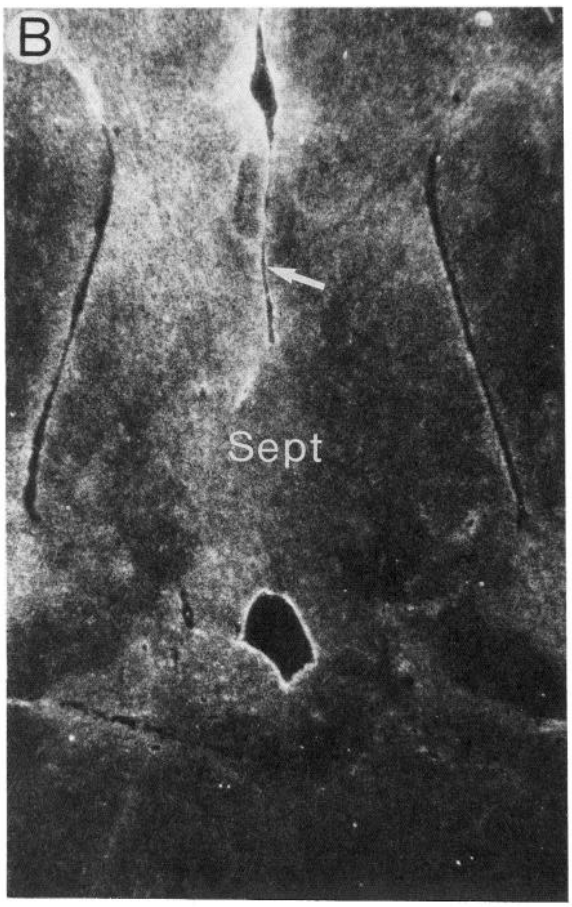
B
Sept

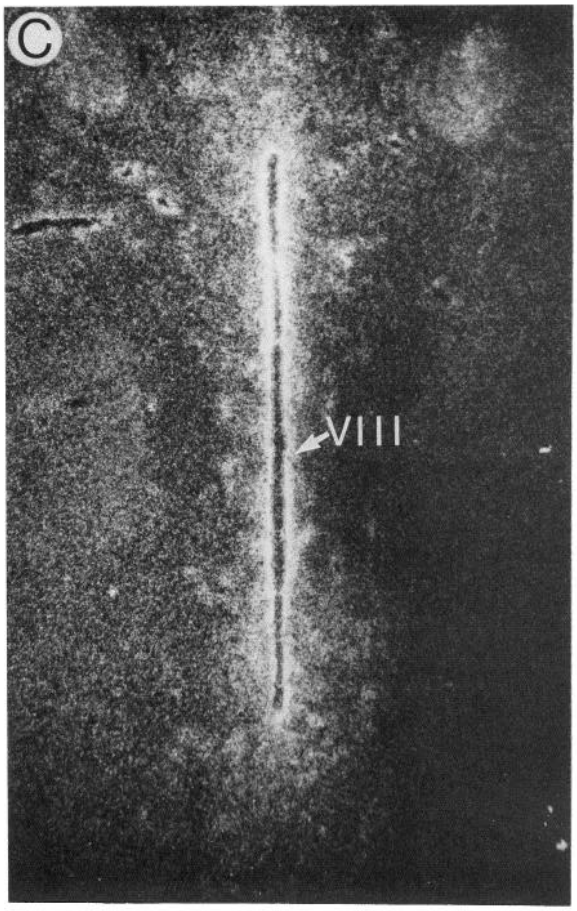
C
VIII

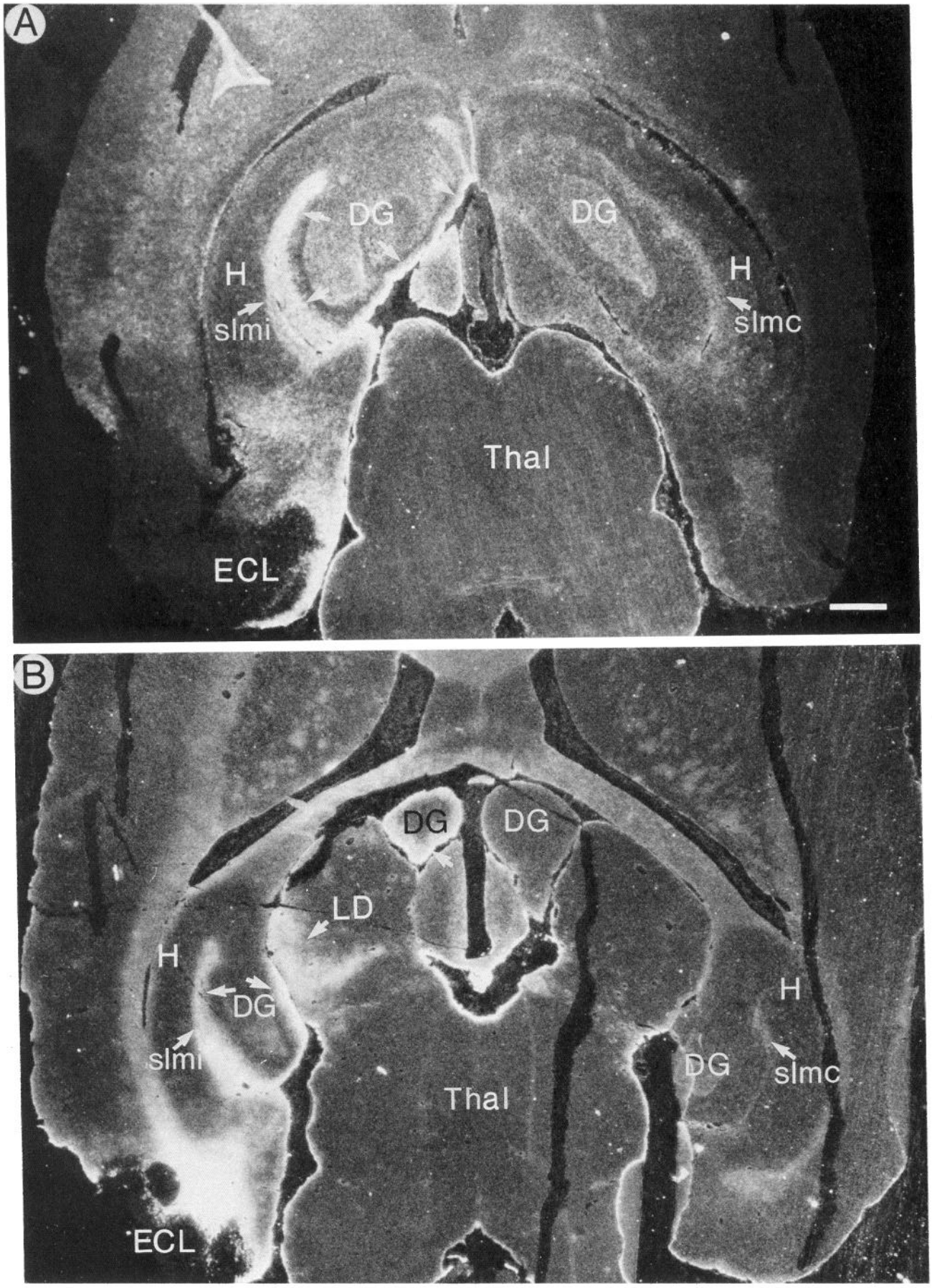
A
DG
DG
H
slmi
H
slmc
Thal
ECL
B
DG
DG
LD
H
DG
slmi
H
DG
slmc
Thal
ECL

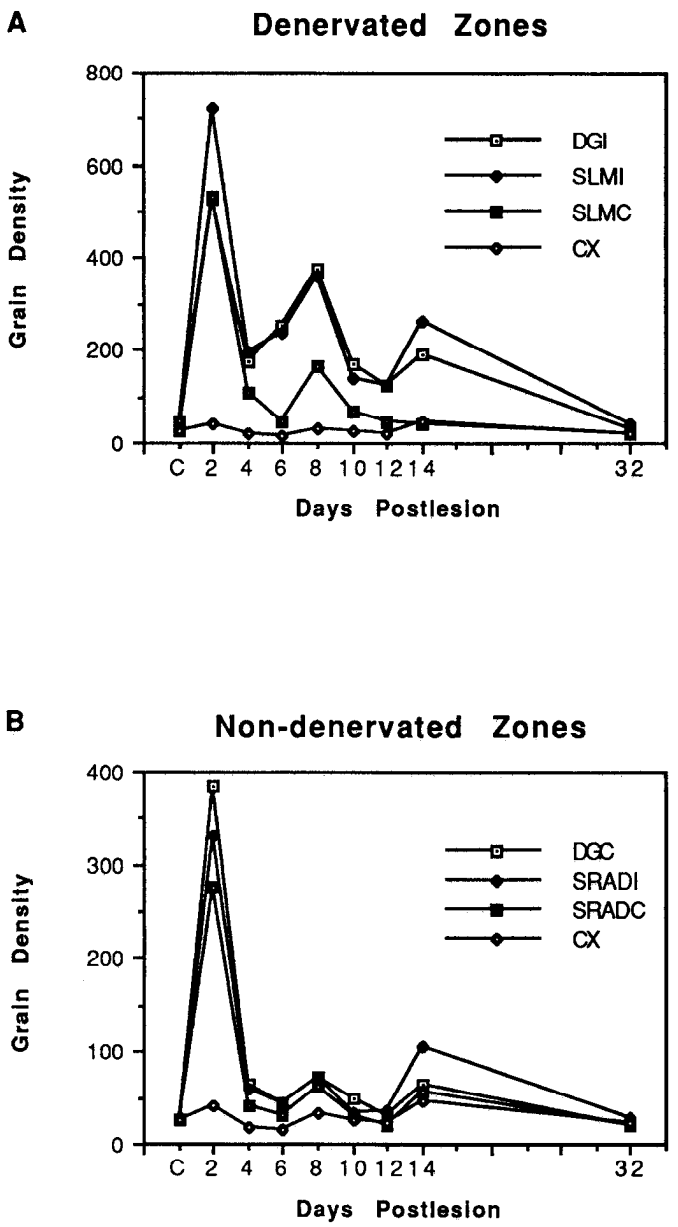

Figure 7. Quantitative analysis of the time course of increases in GFAP mRNA as revealed by *in situ* hybridization. *A,* Average grain density in denervated zones. *DGI* = molecular layer of the dentate gyrus ipsilateral to the lesion; *SLMI* and *SLMC* = stratum lacunosum moleculare of the CA1 region ipsi- and contralateral to the lesion. *CX* = cortex. *B,* Average grain density in nondenervated zones. *DGC* = molecular layer of the dentate gyrus contralateral to the lesion. *SRADI* and *SRADC* = stratum radiatum of the CA1 region ipsi- and contralateral to the lesion. *CX* = cortex. Averaging across measuring sites and postlesion intervals, the average standard deviation of the measurements from the different slides from a single animal was 24.5% of the respective means. The average range of the measurements from the 2 animals at each time point was 13.6% of the respective means. There was no tendency for these measurements of variability to be different at the different measuring sites or across the postlesion interval.

In each setting, the potential signals that might lead to increases in GFAP production are different.

The reactive changes in glia that occur at the site of injury could be set into motion by any of a number of factors related to the injury itself, including degeneration debris, mechanical changes in the tissue, ionic changes, or disruption of the blood-brain barrier (for a recent discussion, see Mathewson and Berry, 1985). The potential signals that lead to increased production of GFAP in areas undergoing retrograde or orthograde degeneration are more limited. In these settings, it is usually thought that glial reactivity is related to the presence of degeneration debris.

Given previous work, the increases in the levels of GFAP mRNA within the denervated zones in the hippocampus are not surprising. Previous studies of glial morphology after unilateral entorhinal cortex lesions have documented a reactive glial response within the denervated hippocampus which begins within 1–2 d postlesion (Rose et al., 1976). In addition, immunocytochemical studies have demonstrated substantial increases in GFAP within astrocytes in the denervated dentate gyrus (Gage et al., 1988). However, the dramatic increase in GFAP mRNA in the nondenervated zones ipsilateral and contralateral to the lesion at 2 d postlesion and the increases in GFAP mRNA in periventricular zones suggest a signal for reactive gliosis that does not involve degeneration debris. These unexpected results will be considered first.

Increases in GFAP mRNA in nondenervated zones

The present results reveal that there are dramatic increases in GFAP mRNA throughout the hippocampus in zones where previous studies using highly sensitive silver impregnation methods have revealed little or no degeneration debris. Moreover, increases in labeling were also observed over the surface of the tectum and in periventricular regions. Within the hippocampus, the increases in areas that do not receive direct projections from the entorhinal cortex were most apparent at 2 d postlesion and were not noticeable thereafter. However, the increases in labeling over periventricular zones persisted throughout the 2–14-d postlesion interval.

The increases in GFAP mRNA in areas that do not contain degenerating processes must occur in response to some signal other than degeneration debris. Possibilities for the signal that leads to the transient upregulation of GFAP message at a distance from the lesion include: (1) release of a diffusible substance that affects glial cells over a widespread area, and (2) changes in activity produced by the lesion (transient increases in activity at the time of the electrolytic lesion or persistent decreases in cellular activity thereafter).

In the case of the increases in GFAP mRNA in the periventricular areas and over the surface of the tectum, a diffusible factor seems most likely. A diffusible factor would presumably be produced at the site of injury or within areas that receive direct projections from the damaged regions and would diffuse throughout the ventricular system. One would expect the effect of a diffusible factor to be most pronounced in periventricular areas, and to decrease with distance from the site of production. This is essentially the pattern that was observed. In this regard, it is of considerable interest that the production of astrocyte mitogenic and morphogenic factors is substantially increased after entorhinal cortical lesions, and that these diffusible agents can be harvested by placing gel foam implants at the site of the injury (Nieto-Sampedro et al., 1985).

There is a problem with the hypothesis that the increases in GFAP mRNA result from increases in the production of astrocyte mitogenic and morphogenic factors at the site of injury. The most dramatic increases in GFAP mRNA were observed at the earliest postlesion interval examined (2 d postlesion). However, the increases in mitogenic and morphogenic

factors have been reported to develop gradually after the lesions, reaching a peak only after several days (Nieto-Sampedro et al., 1985). In fact, the peak concentration of these factors seems to be at 10–15 d postlesion. Resolution of these inconsistencies will likely require identification of the specific factors involved.

One candidate for a diffusible factor that affects astrocytes is interleukin. The production of agents that behave similarly to interleukins 1 and 2 is substantially increased after entorhinal cortical lesions (Nieto-Sampedro and Berman, 1988; Nieto-Sampedro and Chandy, 1987). Both interleukin-like molecules can be harvested from gel foam implants into the lesion site, and both have mitogenic effects on brain astrocytes (Nieto-Sampedro and Berman, 1988; Nieto-Sampedro and Chandy, 1987). In addition, interleukin-1 increases GFAP production in astrocytes (Giulian et al., 1988b) and may act as an astroglial growth factor (Giulian et al., 1988a). Increased production of interleukin at the lesion site would lead to a diffusion of the molecules throughout the ventricular system. Increased production of interleukins would thus be expected to lead to the types of increased production of GFAP that we observed. Again, however, the maximal increases in interleukin-like molecules occur somewhat later than the maximal increases in GFAP mRNA.

In the case of the increases in GFAP mRNA within the nondenervated zones in the hippocampus, the potential signals are less clear. Again, the increases in labeling for GFAP mRNA at early postlesion intervals in these areas did not correspond directly with areas that would contain terminal degeneration. For example, in the hippocampus, the increases occurred bilaterally, even at a considerable distance from the lesion. However, in contrast to the labeling in periventricular zones and over the tectum, the increases in labeling were evident throughout the depth of the affected structures. In particular, there was no evidence of a gradient with distance from the ventricular surface. In addition, on the side contralateral to the lesion, there were large increases in labeling over the hippocampus, while adjacent areas of the tectum and diencephalon showed little or no increase in labeling except at the ventricular surface (see Fig. 5). In these respects, the pattern of increased labeling in the hippocampus is different than would be expected in response to some diffusible agent in the ventricular system.

It has also been suggested that increased synthesis of GFAP by astrocytes is induced by a factor secreted by activated microglia (Gage et al., 1988). This hypothesis is based on previous studies which reveal that: (1) activated microglia secrete a substance that stimulates astrocyte proliferation (Giulian and Baker, 1985), and (2) entorhinal lesions lead to a proliferation of microglia in the hippocampus (Gall et al., 1979). Interestingly, the microglia that proliferate after the lesion appear bilaterally within the hippocampus and are found in both denervated and nondenervated zones. These results would thus be consistent with the hypothesis that activated microglia secrete a substance that stimulates the production of GFAP mRNA in astrocytes.

Again, the problem with this hypothesis is the relationship between microglial proliferation and the increases in mRNA for GFAP. The proliferation of microglia occurs between 24 and 36 hr postlesion (Gall et al., 1979). However, by 24 hr postlesion, GFAP mRNA levels are already near maximal. This temporal relationship would suggest that both microglial proliferation and the induction of GFAP mRNA are regulated by some other signal.

The increases in labeling within the hippocampus that cannot easily be accounted for by the action of a diffusible agent or as a result of an induction of GFAP synthesis by activated microglia do occur within areas in which one would expect activity to be affected. For example, electrolytic lesions presumably produce transient seizure activity over widespread areas. Over the longer term, it is known that neuronal activity is dramatically reduced in the ipsilateral dentate gyrus for several days following a unilateral entorhinal cortical lesion (Reeves and Steward, 1988). The granule cells project to CA3, which in turn gives rise to bilateral projections to CA1. Thus, unilateral lesions of the entorhinal cortex will presumably disrupt activity bilaterally in the hippocampus. Thus, the increases in GFAP mRNA might occur in response to the transient increase in activity that occurs during the lesion, or in response to the decreases in activity that persist for days following the lesion. The latter hypothesis is consistent with studies in the auditory system, which reveal dramatic alterations in glial cells following blockade of afferent activity with TTX (Canady and Rubel, 1989). It remains possible, however, that some diffusible signal is induced which affects glia differently within particular brain regions (the hippocampus vs. other brain regions). Further studies will be required to evaluate these possibilities.

Increases in GFAP mRNA within the denervated zones

The persistent increases in the levels of GFAP mRNA within the denervated zones *do* occur in areas containing degeneration debris; thus, these persistent increases may reflect a glial response induced by degeneration. It is also possible, however, that the increases are *induced* by the same signals that lead to upregulation of GFAP mRNA production within nondenervated zones, but are *maintained* by the presence of degeneration debris or some locally acting signal from the denervated neurons.

Relationship between the increases in GFAP mRNA and the increases in protein synthesis within the denervated zones

One important issue is whether the increased synthesis of GFAP accounts for the increases in protein synthesis within the denervated zones. Here, the answer is not clear. On the one hand, the time course of the increases in mRNA levels does not correspond to the time course of the increases in synthesis. The increases in mRNA levels are most pronounced at 1–2 d postlesion; the increases in synthesis are maximal at 6–8 d and are not apparent at 1–2 d postlesion. However, the increases in GFAP mRNA levels may not be tightly coupled to the increases in GFAP synthesis. Thus, it is possible that the increases in GFAP synthesis are delayed with respect to the increases in GFAP mRNA, and that levels of synthesis are actually maximal during the 6–8-d postlesion interval. However, immunocytochemical studies reveal that there is a substantial increase in GFAP in the dentate gyrus within 4 d after unilateral entorhinal lesions (Gage et al., 1988). Intermediate time points were not evaluated in this study. These results suggest that it is unlikely that the maximal synthesis of GFA protein occurs at 8 d postlesion. Thus, the weight of evidence favors the interpretation that increases in GFAP synthesis do not account for all of the increase in protein synthesis within the denervated zone.

In addition to providing insights into the molecular processes that play a role in reactive gliosis, the present results also provide an important data base for future studies of changes in gene expression in the denervated hippocampus after injury. The process of reactive synaptogenesis has been well characterized

in the hippocampus (Steward and Vinsant, 1983), providing a potentially important model system in which to explore changes in gene expression associated with synapse reorganization (Steward, 1986). However, in order to evaluate changes in unidentified gene transcripts that might be involved in growth processes, it will be important to have a positive control to document that known changes in gene expression can be detected. The present results provide the data base for such a positive control.

References

Amaducci L, Forno KI, Eng LF (1981) Glial fibrillary acidic protein in cryogenic lesions of the rat brain. Neurosci Lett 21:27–32.

Ausubel FM, Brent R, Kingstone RE, Moore DD, Smith JA, Seidman JG, Struhl K (1987) Current protocols in molecular biology. New York: Greene Publishing Associates and Wiley-Interscience.

Barret CP, Guth L, Donati EJ, Krikorian JG (1981) Astroglial reaction in the grey matter of lumbar segments after mid-thoracic transection of the adult rat spinal cord. Exp Neurol 73:365–377.

Bignami A, Dahl D (1976) The astroglial response to stabbing. Immunofluorescence studies with antibodies to astrocyte specific protein (GFA) in mammalian and sub-mammalian vertebrates. Neuropathol Appl Neurobiol 2:99–110.

Burry RW (1983) Antimitotic drugs that enhance neuronal survival in olfactory bulb cultures. Brain Res 261:261–275.

Caceres A, Binder LI, Payne MR, Bender P, Rebhun L, Steward O (1983) Differential subcellular localization of tubulin and the microtubule-associated protein MAP2 in brain tissue as revealed by immunocytochemistry with monoclonal hybridoma antibodies. J Neurosci 4:394–410.

Canady KS, Rubel EW (1989) Rapid proliferation of astrocytic processes in chick cochlear nucleus following afferent activity blockade. Neurosci Abstr 15:512.

Chirgwin JM, Przybyla AE, MacDonald J, Rutter W (1979) Isolation of biologically active ribonucleic acid from sources enriched in ribonuclease. Biochemistry 18:5294–5299.

Cook RD, Wisniewski HM (1973) The role of oligodendroglia and astroglia in Wallerian degeneration of the optic nerve. Brain Res 61: 191–206.

Cotman CW, Nadler JV (1978) Reactive synaptogenesis in the hippocampus. In: Neuronal plasticity (Cotman CW, ed), pp 227–271. New York: Raven.

Fass B, Steward O (1983) Increases in protein precursor incorporation in the denervated neuropil of the dentate gyrus during reinnervation. Neuroscience 9:633–664.

Gage FH, Olejniczak P, Armstrong DM (1988) Astrocytes are important for sprouting in the septohippocampal circuit. Exp Neurol 102:2–13.

Gall C, Rose G, Lynch G (1979) Proliferative and migratory activity of glial cells in the partially deafferented hippocampus. J Comp Neurol 183:539–550.

Giulian D, Baker TJ (1985) Peptides released by amyboid microglia regulate astrocyte proliferation. J Cell Biol 101:2411–2415.

Giulian D, Young DG, Woodward J, Brown DC, Lachman LB (1988a) Interleukin-1 is an astroglial growth factor in the developing brain. J Neurosci 8:709–714.

Giulian D, Woodward J, Young DG, Krebs JF, Lachman LB (1988b) Interleukin-1 injected into mammalian brain stimulates astrogliosis and neovascularization. J Neurosci 8:2485–2490.

Graeber MB, Kreutzberg GW (1986) Astrocytes increase in glial fibrillary acidic protein during retrograde changes of facial motor neurons. J Neurocytol 15:363–373.

Holmes E, Hermanson G, Cole R, de Vellis J (1988) Developmental expression of glial-specific mRNAs in primary cultures of rat brain visualized by *in situ* hybridization. J Neurosci Res 19:389–396.

Lawrence JB, Singer RH (1986) Intracellular localization of messenger RNAs for cytoskeletal proteins. Cell 45:407–415.

Lewis SA, Balcarek JM, Krek V, Shelanski M, Cowan NJ (1984) Sequence of a cDNA clone encoding mouse glial fibrillary acidic protein: structural conservation of intermediate filaments. Proc Natl Acad Sci USA 81:2743–2746.

Loesche J, Steward O (1977) Behavioral correlates of denervation and reinnervation of the hippocampal formation of the rat: recovery of alternation performance following unilateral entorhinal cortical lesions. Brain Res Bull 2:31–40.

Maniatis T, Fritchs EF, Sambrook J (1983) Molecular cloning. A laboratory manual, 6th ed. Cold Spring Harbor, NY: Cold Spring Harbor Laboratory.

Mathewson AJ, Berry M (1985) Observations on the astrocyte response to a cerebral stab wound in adult rats. Brain Res 327:61–69.

Matthews DA, Cotman C, Lynch G (1976) An electron microscopic study of lesion-induced synaptogenesis in the dentate gyrus of the adult rat. I. Magnitude and time course of degeneration. Brain Res 115:1–21.

Nathaniel EH, Nathaniel DR (1981) The reactive astrocyte. Adv Cell Neurobiol 2:249–301.

Needels DL, Nieto-Sampedro M, Wittemore SR, Cotman CW (1986) Induction of a neurite-promoting factor in rat brain following injury or deafferentation. Neuroscience 18:517–526.

Nieto-Sampedro M, Berman MA (1988) Interleukin-1-like activity in rat brain: sources, targets, and effects of injury. J Neurosci Res 17: 214–219.

Nieto-Sampedro M, Chandy KG (1987) Interleukin-2-like activity in injured rat brain. Neurochem Res 12:723–727.

Nieto-Sampedro M, Lewis ER, Cotman CW, Manthorpe M, Skaper SD, Barbin G, Longo FM, Varon S (1982) Brain injury causes a time-dependent increase in neuronotrophic activity at the lesion site. Science 217:860–861.

Nieto-Sampedro M, Manthorpe M, Barbin G, Varon S, Cotman CW (1983) Injury-induced neuronotrophic activity in adult brain: correlation with survival of delayed implants in the wound cavity. J Neurosci 3:2219–2229.

Nieto-Sampedro M, Saneto RP, de Vellis J, Cotman CW (1985) The control of glial populations in brain: changes in astrocyte mitogenic and morphogenic factors in response to injury. Brain Res 343:320–328.

Phillips LL, Nostrandt SJ, Chikaraishi DM, Steward O (1987) Increases in ribosomal RNA within the denervated neuropil of the dentate gyrus during reinnervation: evaluation by *in situ* hybridization using DNA probes complementary to ribosomal RNA. Mol Brain Res 2:251–261.

Reeves TM, Steward O (1988) Changes in the firing properties of neurons in the dentate gyrus with denervation and reinnervation: implications for behavioral recovery. Exp Neurol 102:37–49.

Rose G, Lynch G, Cotman CW (1976) Hypertrophy and redistribution of astrocytes in the deafferented dentate gyrus. Brain Res Bull 1:87–92.

Rosenthal A, Chan SY, Henzel W, Haskell C, Kuang W-J, Chen E, Wilcox JN, Ullrich A, Goeddel DV, Routtenberg A (1987) Primary structure and mRNA localization of protein F1, a growth-related protein kinase C substance associated with synaptic plasticity. EMBO J 6:3641–3646.

Schiffer D, Giordana MT, Migheli A, Giaccone G, Pezzatta S, Mauro A (1986) Glial fibrillary acidic protein and vimentin in the experimental glial reaction of the rat brain. Brain Res 374:110–118.

Steward O (1983) Alterations in polyribosomes associated with dendritic spines during the reinnervation of the dentate gyrus of the adult rat. J Neurosci 3:177–188.

Steward O (1986) Lesion-induced synapse growth in the hippocampus: in search of cellular and molecular mechanisms. In: The Hippocampus (Isaacson RL, Pribram KH, eds). pp 65–111. New York: Plenum.

Steward O, Vinsant SV (1983) The process of reinnervation in the dentate gyrus of the adult rat. A quantitative electron microscopic analysis of terminal proliferation and reactive synaptogenesis. J Comp Neurol 214:370–386.

Steward O, Cotman CW, Lynch G (1974) Growth of a new fiber projection in the brain of adult rats: reinnervation of the dentate gyrus by the contralateral entorhinal cortex following ipsilateral entorhinal lesions. Exp Brain Res 20:45–66.

Tetzlaff W, Graeber MB, Bisby MA, Kreutzberg GW (1988) Increased glial fibrillary acidic protein synthesis in astrocytes during retrograde reaction of the rat facial nucleus. Glia 1:90–95.

Vaughn JE, Hinds PL, Skoff RP (1970) Electron microscopic studies of Wallerian degeneration in the optic nerve of the rat. I. The multipotential glia. J Comp Neurol 140:175–206.

Wahl GM, Ong E, Meinkoth J, Franco R, Barinaga M (1981) Methods for the transfer of DNA, RNA, and protein to nitrocellulose and diazotized paper solid supports. Keene, NH: Scleicher and Schuell.